IMWA 2026
Jeongseon

Multi-Temporal UAV Hyperspectral Monitoring of a Mine-Water Influenced Pond System: Harpener Teiche (Germany)

Hernan Flores[1,2], Barbara M.A. Teichert[1], Simon Nikutta[1], Tobias Rudolph[1]

[1]*Research Center of Post-Mining, University of Applied Sciences Georg Agricola (THGA), Herner Straße 45, 44787 Bochum, Germany*

[2]*Institute of Mine Surveying and Geodesy, TU Bergakademie Freiberg, Fuchsmühlenweg 9B, 09599 Freiberg, Germany*

Correspondence author: hernan.flores@thga.de

Abstract

This study evaluates UAV-based hyperspectral imaging for multi-temporal monitoring of a mine-water influenced pond system at Harpener Teiche, Bochum, Germany. Three campaigns between October 2025 and February 2026 were processed to reflectance and analysed using a normalized four-band VNIR brightness metric. The resulting maps and transect profiles reveal recurrent optical patterns associated with the mine-water inflow and plume dispersion. Spectral reflectance profiles distinguish optical signatures of inflow, mixing zone, and background pond water, while in-situ electrical conductivity and temperature measurements provide hydrochemical context. The approach complements point-based monitoring with spatially continuous observations.

Keywords: UAV; hyperspectral sensing; mine-water; environmental monitoring; post-mining; remote sensing

Introduction

Mine-water discharge is one of the most persistent environmental challenges associated with the legacy of underground mining. After mine closure, active water management is required to prevent groundwater rebound and flooding of underground workings, resulting in large volumes of mine-water being continuously pumped and discharged into nearby rivers, streams, or artificial lakes.

Conventional monitoring of these discharges relies on in-situ sampling and laboratory analysis, which provide detailed chemical information but are limited to discrete sampling points. Consequently, spatial patterns and mixing processes within receiving water bodies often remain poorly characterized. Remote sensing offers complementary capabilities: hyperspectral imaging provides near-continuous spectral information across many narrow bands, while recent advances in uncrewed aerial vehicle (UAV) platforms enable flexible, high-resolution deployment over targeted areas. Previous studies have demonstrated the potential of UAV-based hyperspectral sensing for monitoring aquatic environments affected by acid mine drainage (Flores *et al.*, 2021), mine-water sludge in tailings ponds (Flores *et al.*, 2024), and variations in water optical properties related to turbidity and mixing processes (Cui *et al.*, 2022). However, its application for tracking environmental changes on a multi-temporal basis remains limited.

In this study, we evaluate the capability of UAV-based hyperspectral imaging for multi-temporal monitoring of a mine-water influenced pond system at Harpener Teiche (Bochum, Germany). By integrating UAV hyperspectral imagery with in-situ water measurements, the study demonstrates how high-resolution remote sensing can complement conventional monitoring and improve the understanding of spatial environmental processes within mine-water systems.

Study Area

The study area is located at Harpener Teiche (Fig. 1), a system of artificial ponds situated in the city of Bochum within the Ruhr mining region in western Germany. The ponds form part of a local surface water system influenced by historical coal mining activities in the region.

Previous studies have shown that mine-water inflows represent a major component of the water balance in the Harpener Teiche and the downstream hydrological

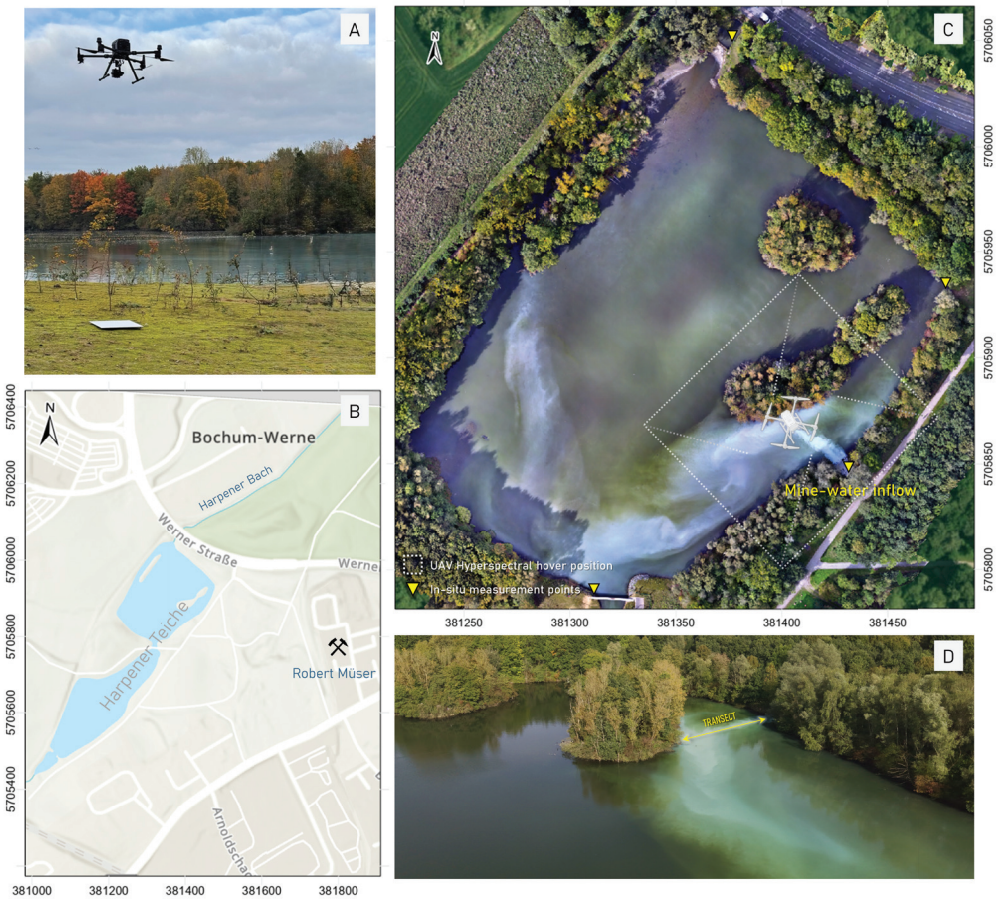

Figure 1 Study area and UAV monitoring configuration at Harpener Teiche (Bochum, Germany). (A) UAV system used for hyperspectral data acquisition. (B) Location within Bochum. (C) UAV orthomosaic showing the mine-water inflow, hover acquisition area, and in-situ measurement points (yellow markers). (D) Oblique image of the visible plume and the A–B transect used for spatial analysis. Coordinates in panels B and C: ETRS89 / UTM Zone 32N (EPSG:25832), in meters.

network (Schneider *et al.*, 2008). The discharged mine-water originates from the former Robert Müser coal mine and is characterized by elevated mineralization, increased temperature, and sulfur-related treatment products, which influence the physical and chemical conditions of the receiving water body. In the present field campaigns, electrical conductivity measured near the mine-water inflow ranged between approximately 5.36 and 5.87 mS cm^{-1}, while water temperature ranged between 17.9 and 20.4 °C. These values are consistent with a highly mineralized mine-water influence. Sulfur species were not quantified in this study; however, the whitish coloration of the inflow is linked to the mine-water treatment process, where hydrogen peroxide is added to oxidize hydrogen sulfide. This process can produce sulfur-related suspended particles that contribute to the visible plume.

The Harpener Teiche system consists of two main shallow artificial ponds connected to a small stream network (Fig. 1B). Mine-water is discharged into the pond through a controlled inflow structure connected to the regional mine-water management infrastructure (Fig. 1C). The inflow generates a visible plume within the pond due to differences in turbidity and suspended particles, likely including sulfur-related treatment products, between mine-water and the surrounding pond water (Fig. 1D).

Aerial and field measurements were collected during three monitoring campaigns in October 2025, December 2025, and February 2026. During each campaign, in-situ measurements of water temperature, electrical conductivity (EC), and pH were obtained at four accessible shoreline locations within the pond system, including the mine-water inflow area and three additional points around the pond. These locations are indicated by yellow markers in Fig. 1C. Water parameters were measured using a multi-parameter portable meter (WTW ProfiLine Multi 3320). The pH meter was calibrated using Hanna standard solutions (pH 4.01 and pH 7.01). The probes were placed directly into the water from the shoreline with gentle agitation, and measurements were recorded once the readings stabilized.

Methods

UAV hyperspectral data acquisition

Hyperspectral data were collected using a UAV-mounted BlackBird V2 hyperspectral camera (HAIP Solutions GmbH, 2022) operating in the visible to near-infrared (VNIR) spectral range. The sensor was mounted on a DJI Matrice M350 RTK platform (Fig. 1A) and includes a hyperspectral (HSI) sensor and a separate RGB camera for livestreaming on the remote controller. The hyperspectral sensor captures images at a native resolution of 540 × 540 pixels and records 100 spectral bands across the 500–1000 nm wavelength range, with a spectral resolution and spectral sampling interval of 5 nm according to the manufacturer specifications. The sensor was deployed in a hover acquisition configuration above the mine-water inflow zone to maximize spatial resolution and minimize geometric distortions. The UAV was operated at a flight height of 120 m above ground level with constant sensor orientation, resulting in an approximate ground sampling distance of 0.13 m per pixel. Georeferencing was based on the integrated positioning system of the RTK-enabled UAV platform. Camera settings were adjusted slightly between campaigns to account for changing illumination conditions.

Hyperspectral preprocessing

Hyperspectral datasets were preprocessed using a custom Python-based preprocessing workflow developed by the first author, comprising dark frame correction, radiometric calibration, reflectance calibration using a reference panel, and spectral smoothing. A water mask was applied to isolate the pond surface and exclude surrounding vegetation and land areas from the analysis.

To compare spatial patterns between campaigns, a four-band brightness metric was calculated as the arithmetic mean of reflectance at 557, 667, 752, and 852 nm. These wavelengths were selected to represent visible, red-edge, and near-infrared regions sensitive to suspended particles, turbidity-related scattering, and plume visibility, while avoiding major atmospheric and water absorption features near 760 nm and 970 nm (Wu *et al.*, 2014; Cui *et al.*, 2022). The metric

was used as a relative brightness proxy, not as a physically based turbidity index. Brightness values were then normalized to a 0–1 range using min–max scaling.

Results

Multi-temporal hyperspectral monitoring

Normalized brightness maps derived from the hyperspectral datasets reveal a recurrent optical pattern associated with the mine-water inflow during the three monitoring campaigns. In all datasets, the inflow area is characterized by increased normalized brightness relative to the surrounding pond water, indicating enhanced reflectance linked to suspended particles, turbidity-related effects, and plume dispersion.

Figure 2 illustrates the spatial distribution of normalized brightness values across the water surface during the three monitoring dates. The brightness maps consistently identify the mine-water inflow and the associated plume-like dispersion pattern. While the exact spatial extent and intensity of the high-brightness zone vary between campaigns, the inflow signature remains detectable in all three datasets. These variations likely reflect differences in illumination, local hydrodynamic conditions, and short-term mixing behaviour at the time of acquisition.

The repeated detection of this optical anomaly demonstrates that UAV hyperspectral imagery can capture spatial patterns related to mine-water dispersion within the pond system. The brightness metric should therefore be interpreted as a relative optical proxy for plume visibility and turbidity-related spatial variability, rather than as a direct measurement of water chemistry.

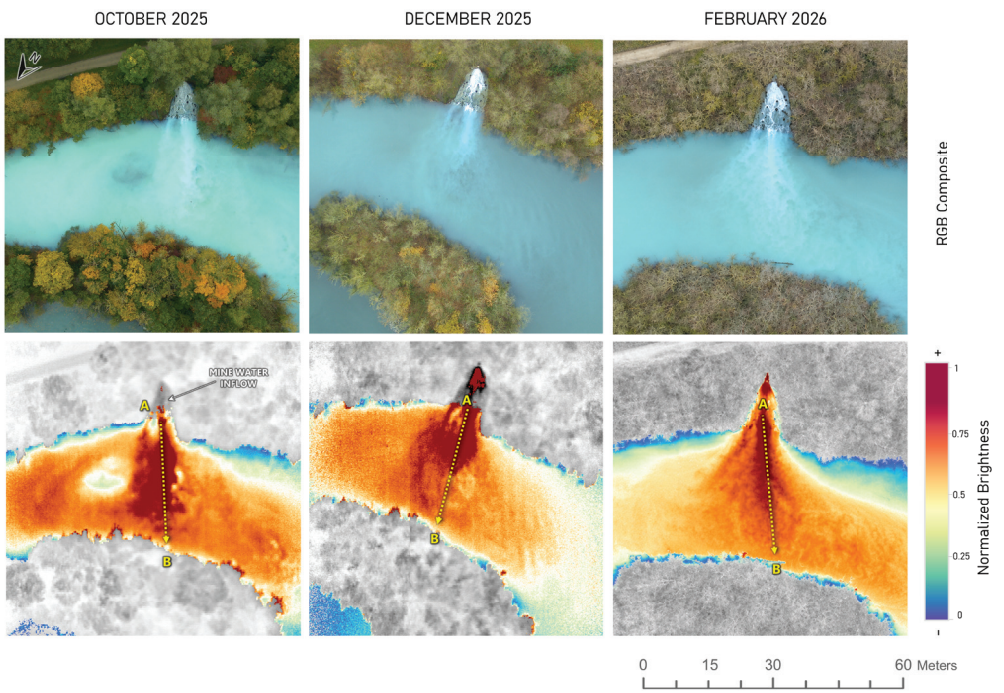

Figure 2 *Multi-temporal UAV monitoring of the mine-water inflow at Harpener Teiche. The upper row shows RGB composites acquired during the October 2025, December 2025, and February 2026 campaigns. The lower row shows min–max normalized hyperspectral brightness maps derived from selected VNIR bands. The A–B transects indicate the plume-axis profiles used for the brightness analysis shown in Fig. 3.*

Spatial gradients in optical properties

To quantify spatial variations in brightness across the mixing zone, A–B transects were extracted from the mine-water inflow toward the pond interior for each monitoring campaign, as shown in Figure 2. The resulting profiles in Figure 3 show clear gradients in normalized brightness associated with the transition from the inflow-dominated zone toward areas of lower optical influence.

The brightness profiles show high normalized brightness values near the inflow, corresponding to the visible mine-water plume entering the pond. Along the transect, brightness values generally decrease with distance from the inflow, reflecting changes in water optical properties related to plume dispersion, suspended particles, and mixing with the surrounding pond water.

Differences between the three profiles indicate campaign-specific variations in the spatial extent and intensity of the optical plume. The October profile shows a more gradual decrease along the transect, suggesting a more extended high-brightness zone. In contrast, the December profile decreases more sharply, indicating a more localized optical signal near the inflow. The February profile shows an intermediate pattern, with high brightness near the inflow followed by a progressive decrease toward the pond interior. Overall, these observations indicate that normalized hyperspectral brightness profiles can capture recurring spatial gradients and short-term temporal differences in mine-water plume dispersion under varying environmental conditions.

Spectral reflectance characteristics

Spectral reflectance profiles were extracted from three regions of interest (ROIs) representing the mine-water inflow, the mixing zone, and background pond water (Fig. 4A). The mean spectra show a systematic decrease in reflectance magnitude from the mine-water inflow to the mixing zone and finally to pond water (Fig. 4B). The inflow spectrum exhibits the highest reflectance values across the visible wavelengths, particularly in the green spectral region around 550 nm, which is consistent with increased turbidity and suspended particle concentrations in aquatic environments (Cui *et al.*, 2022). The mixing-zone spectrum

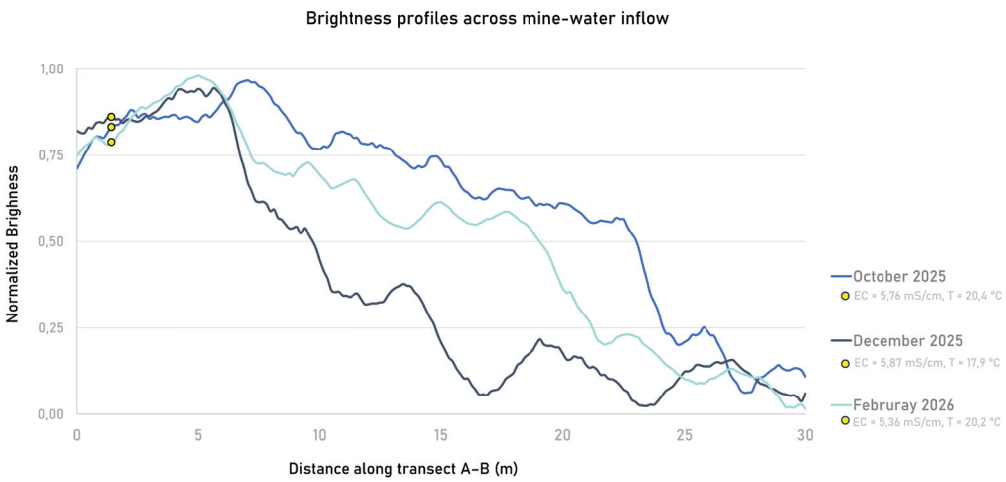

Figure 3 *Normalized brightness profiles extracted along the A–B transects shown in Fig. 2. Distance is measured from the mine-water inflow toward the pond interior over approximately 30 m. All campaigns show a general decrease in normalized brightness away from the inflow, reflecting changes in optical properties across the mixing zone. Yellow markers indicate near-inflow in-situ measurements of electrical conductivity (EC) and water temperature (T), which are shown for hydrochemical context.*

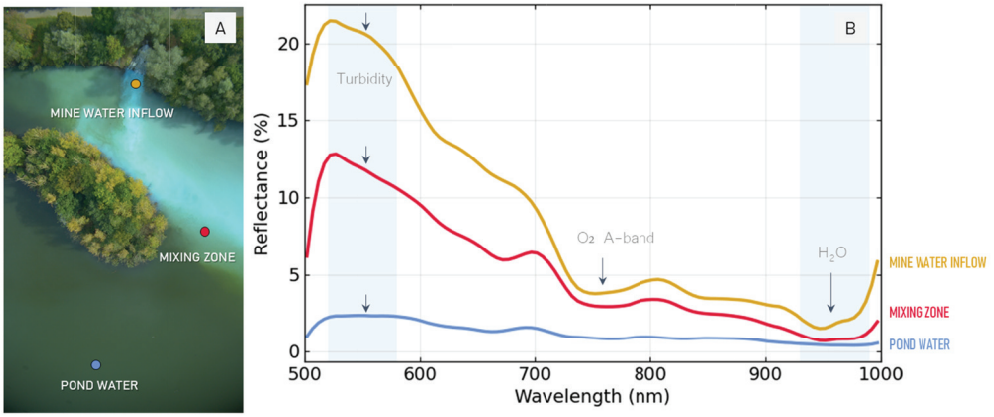

Figure 4 Spectral reflectance profiles from selected regions of interest (ROIs) within the Harpener pond system. (A) Orthoimage showing ROIs for the mine-water inflow, mixing zone, and background pond water. (B) Mean VNIR reflectance spectra (500–1000 nm) extracted from the ROIs. Shaded regions indicate turbidity-sensitive visible wavelengths and atmospheric or water-related absorption features, including the O_2 A-band and H_2O absorption.

shows intermediate reflectance values, while the pond-water spectrum exhibits the lowest overall reflectance.

The spectra are largely featureless across most of the VNIR range, as expected for surface water, but show a narrow absorption feature near 760 nm corresponding to the atmospheric O_2 A-band and a broader decrease around 970 nm associated with liquid-water absorption (Green *et al.*, 2006; Flores *et al.*, 2021). These spectral patterns support the interpretation that the hyperspectral data capture relative optical differences between the inflow, mixing zone, and surrounding pond water, rather than directly measuring water chemistry.

In-situ measurements collected at the four accessible shoreline locations provide hydrochemical context for the hyperspectral observations. Electrical conductivity values measured during the campaigns ranged between approximately 5.3 and 5.9 mS cm^{-1} at the sampled shoreline points, confirming the strong mine-water influence of the pond system. However, because measurements were limited to accessible shoreline locations, these values should not be interpreted as a full spatial validation of electrical conductivity across the pond. In contrast, measurements from the nearby Harpener Bach showed substantially lower electrical conductivity values (< 1 mS cm^{-1}), indicating freshwater primarily derived from precipitation and shallow surface runoff.

Conclusions

This study demonstrates the potential of UAV-based hyperspectral imaging for multi-temporal monitoring of mine-water influenced pond systems. The datasets captured recurrent brightness gradients across the inflow and mixing zone, while spectral reflectance profiles distinguished optical signatures of inflow, mixing zone, and background pond water. In-situ measurements of electrical conductivity and temperature provided hydrochemical context for the mine-water influence at the site.

In practical terms, UAV hyperspectral monitoring can complement conventional sampling by mapping plume extent, guiding sampling locations, and documenting temporal changes in mixing patterns, particularly useful in post-mining water bodies where discharge points are spatially heterogeneous. Future work should exploit the full 100-band dataset and combine UAV observations with denser in-situ measurements collected away from the shoreline, enabling empirical reflectance–turbidity relationships and more quantitative monitoring of mine-water dispersion.

Acknowledgements

The authors thank the Research Center of Post-Mining (FZN), THGA Bochum, for providing the UAV platform and sensor systems, and Dr. Marcin Pawlik for fieldwork support.

References

Cui, M., Sun, Y., Huang, C. and Li, M. 2022. Water turbidity retrieval based on UAV hyperspectral remote sensing. Water, 14(1), 128. https://doi.org/10.3390/w14010128

Flores, H., Lorenz, S., Jackisch, R., Tusa, L., Contreras, I.C., Zimmermann, R. and Gloaguen, R. 2021. UAS-based hyperspectral environmental monitoring of acid mine drainage affected waters. Minerals, 11(2), 182. https://doi.org/10.3390/min11020182

Flores, H., Reker, B., Pawlik, M., Haske, B. and Rudolph, T. 2024. Hyperspectral UAS-sensing for tailing ponds monitoring: Towards responsible resource repurposing. In: Kleinmann, B., Skousen, J. and Wolkersdorfer, C. (eds), Proceedings of the West Virginia Mine Drainage Task Force Symposium & 15th International Mine Water Association Congress, Morgantown, WV, USA, pp. 196–202.

Green, R.O., Painter, T.H., Roberts, D.A. and Dozier, J. 2006. Measuring the expressed abundance of the three phases of water with an imaging spectrometer over melting snow. Water Resources Research, 42. https://doi.org/10.1029/2005WR004509

HAIP Solutions GmbH. 2022. BlackBird V2 hyperspectral camera: Product data sheet. Hannover, Germany.

Schneider, Y., Grube, S. and Weilandt, M. 2008. Determination and evaluation of the phosphorus load of an artificial shallow lake. Water Science and Technology, 58(10), 1993–2000. https://doi.org/10.2166/wst.2008.747

Wu, J.-L., Ho, C.-R., Huang, C.-C., Srivastav, A., Tzeng, J.-H. and Lin, Y.-T. 2014. Hyperspectral sensing for turbid water quality monitoring in freshwater rivers: Empirical relationship between reflectance and turbidity and total solids. Sensors, 14, 22670–22688. https://doi.org/10.3390/s141222670